Acta Polytechnica CTU Proceedings **34**:80–84, 2022
https://doi.org/10.14311/APP.2022.34.0080

Published by the Czech Technical University in Prague

MESH GENERATION AND MECHANICAL TESTS OF BASIC ELEMENT CELLS OF POROUS STRUCTURES

Luboš Řehounek*, Aleš Jíra

Czech Technical University in Prague, Faculty of Civil Engineering, Thákurova 7, 166 29 Prague 6, Czech Republic

* corresponding author: lubos.rehounek@fsv.cvut.cz

Abstract. Advanced porous structures are novel, emerging materials with a broad range of applicability but a rather difficult means of design and manufacturing. The advent and availability of the additive manufacturing industry in the last decade has enabled for production of these structures via 3D printing of polymers and metals. This research deals with the design, mechanical testing and preparation of FEM meshes of novel gyroid structures manufactured by PA12 SLS 3D printing. As demonstrated, conventional means of CAD generation of these structures in the *.STL format are sufficient for manufacture of specimens, but not precise enough for the purpose of mesh generation for FEM due to errors in the geometry of tesselation. Mechanical tests show that the sheet gyroid variant is the preferable geometry as it offers the greatest peak compressive stress among all variants at the same material density.

Keywords: 3D printing, gyroid, porous, mesh, mechanical.

1. Introduction

Osseointegration of implants, which is closely related to the properties of their surfaces and materials, is a topic that has been widely covered in literature and the surface properties of conventional implants today have multiple ways of achieving a good connection at the bone-implant interface (BII). Surface treatment usually aims to roughen the surface of the implant so as to increase its specific surface area. Another approach, made possible by additive manufacturing technologies, is application of a porous surface as an integral part of the geometry. This approach also increases the specific surface of the implant, but not at the level of added material, but rather at level of the implant geometry itself. One such structure is the gyroid, which is also often found in nature [1]. It was first described by the American physicist Alan Schoen in 1970 [2]. The presented mechanical tests show that gyroid structures have very good strength while maintaining very low values of elastic moduli E (a very beneficial characteristic that greatly reduces the stress shielding effect [3–6]) and high porosity. The research shows that for the purpose of manufacturing specimens or real implants, it is acceptable to use a CAD environment for the structure's generation with satisfactory precision of geometry. However, if numerical simulations are considered (FEM), this approach is no longer viable. The gyroid has many forms but it is always a TPMS (triply-period minimal surface) structure with a system of interconnected pores constructed from the sine and cosine functions. An example of TPMS structures is given on Fig. 1.

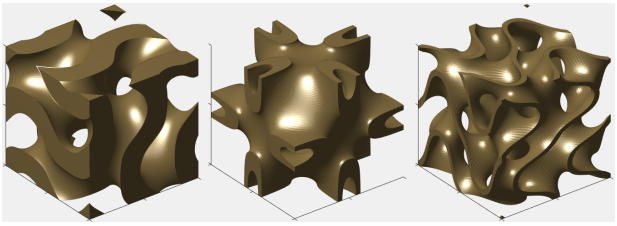

Figure 1. A simple example of TPMS structures. Left – the gyroid structure, middle – the Neovius structure, right – the Fischer-Koch S structure. The structures vary in porosity for demonstration purposes. Generated with MSLattice [7].

2. Materials and Methods

2.1. The Gyroid Structure

The gyroid surface can be approximated with the gyroid equation (Eq. 1). Notably, there are multiple variants of the gyroid structure. The following equation represents the "single gyroid" structure with one solid phase and one void domain:

$$\sin(\overline{x})\cos(\overline{y}) + \sin(\overline{y})\cos(\overline{z}) + \sin(\overline{z})\cos(\overline{x}) = t \quad (1)$$

where a is the length of the edge of a cube that the gyroid structure is circumscribed in, $\overline{x}$, $\overline{y}$ and $\overline{z}$ are modified spatial coordinates so that:

$$\overline{x} = \frac{2\pi x}{a}, \quad \overline{y} = \frac{2\pi y}{a}, \quad \overline{z} = \frac{2\pi z}{a}$$

and t is a parameter that influences the magnitude of the constant curvature of the gyroid structure. By manipulating the values of t, we can achieve variations

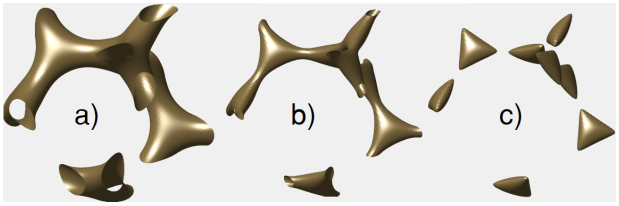

FIGURE 2. Computer-generated (Eq. 1) single gyroid TPMS tubular surfaces with different values of parameter t. Image shows the as-generated surface that needs to be enclosed to create a solid for FEM simulations. Boundary cube has a length of $a = 2\pi$. a) $t = 1.2$, b) $t = 1.38$, c) $t = 1.41$. Parameter t has a domain of $(-1.5; 1.5)$. As we approach the value of $t = 1.5$, the structure begins to lose its typical shape and discontinuities occur.

between the two variants of the structure (*trabecular* beam gyroid system and the gyroid *sheet* system, Fig. 3). However, it has its limitations and the overall shape of the gyroid is very sensitive to its value. For extreme values, discontinuities, deformities and overall loss of shape can be observed (Fig. 2). This approach of generating a TPMS surface is then followed by enclosing one domain (either the trabecular or the sheet domain) to create the desired partition. Notably, a gyroid structure created as such always lends to the ability to create either partition as the process of creating the solid from the TPMS surface always leads to decomposition of a circumsscribed cube into two (in case of the single gyroid Eq. 1) separate domains. Therefore, the other partition (domain) is always in a geometrically inverse relationship to the other in a circumscribed cube (Fig. 4).

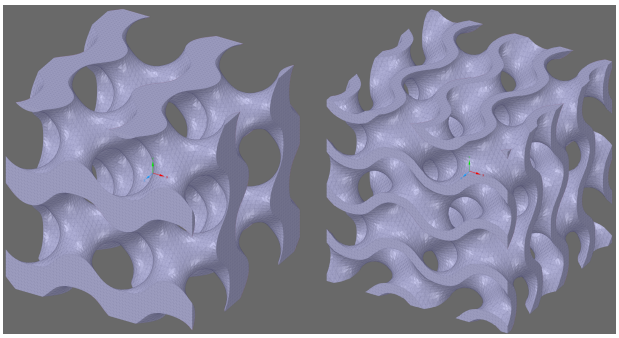

FIGURE 3. Two variants of the single gyroid structure. Left – the trabecular system (sometimes referred to as the *tubular* system), right – the sheet system. The properties of the gyroid can be manipulated by the parameter t, which determines the final appearance of the structure and the character of the system (trabecular, sheet or a fluid combination). Structures have different porosities for purpose of clear demonstration.

Another variant of the gyroid structure is the Double gyroid, represented by Eq. 2.

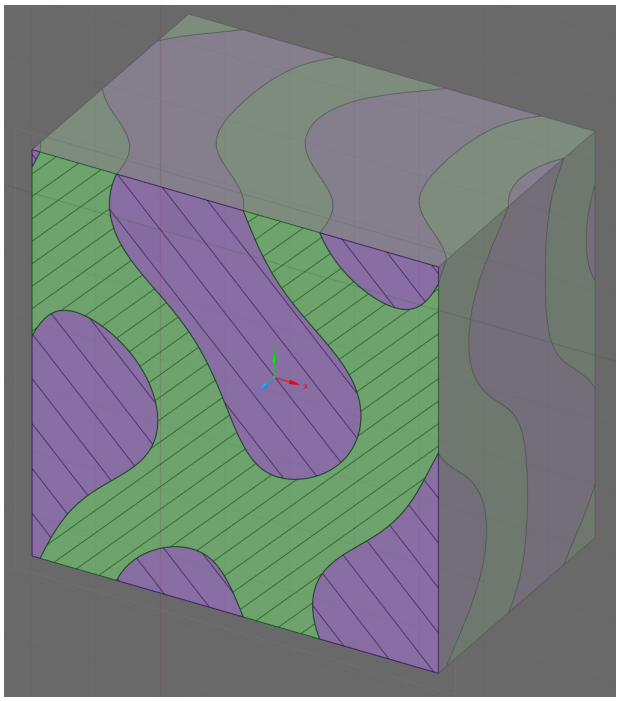

.

FIGURE 4. A section showing the inverse relationship between the two partitions of a circumscribed cube in which a gyroid structure is generated. If a structure is generated from a TPMS function equation (Eq. 1 or Eq. 2), the other domain will always be an inverse gyroid structure with a different t value. On this picture, purple color represents the trabecular (tubular) gyroid and green represents the sheet gyroid. Note that the differences in appearance of either partition are influenced by the parameter t (Eq. 1)

$$\Big[\sin(\overline{x})\cos(\overline{y}) + \sin(\overline{y})\cos(\overline{z}) + \sin(\overline{z})\cos(\overline{x})\Big]^2 = t^2 \tag{2}$$

where a, $\overline{x}$, $\overline{y}$, $\overline{z}$ and t have the same meaning as in Eq. 1.

Another important property of the gyroid structure is its chirality. Therefore, it is asymmetric and cannot be created or generated by mirror or translation operations. A gyroid basic element cell cannot be divided along any axis or plane and superimposed on itself [8].

2.2. Mechanical Tests

The specimens for mechanical tests were made in the Autodesk NetFabb software as single gyroid porous structures with dimensions of 25.12×25.12×25.12 mm. The specimens also had a top and bottom homogeneous plate fitted for a more uniform load distribution. The height of this plate was set to 2 mm. Three variants of structures were manufactured, each with a porosity of $n = 0.75$. The variants were the Dode-Thick structure, sheet gyroid with a defined wall thickness of 0.5 mm and a trabecular gyroid with parameter value $t = 0.78$. The gyroid structures were made using Eq. 1 with a period of 2π. The sheet

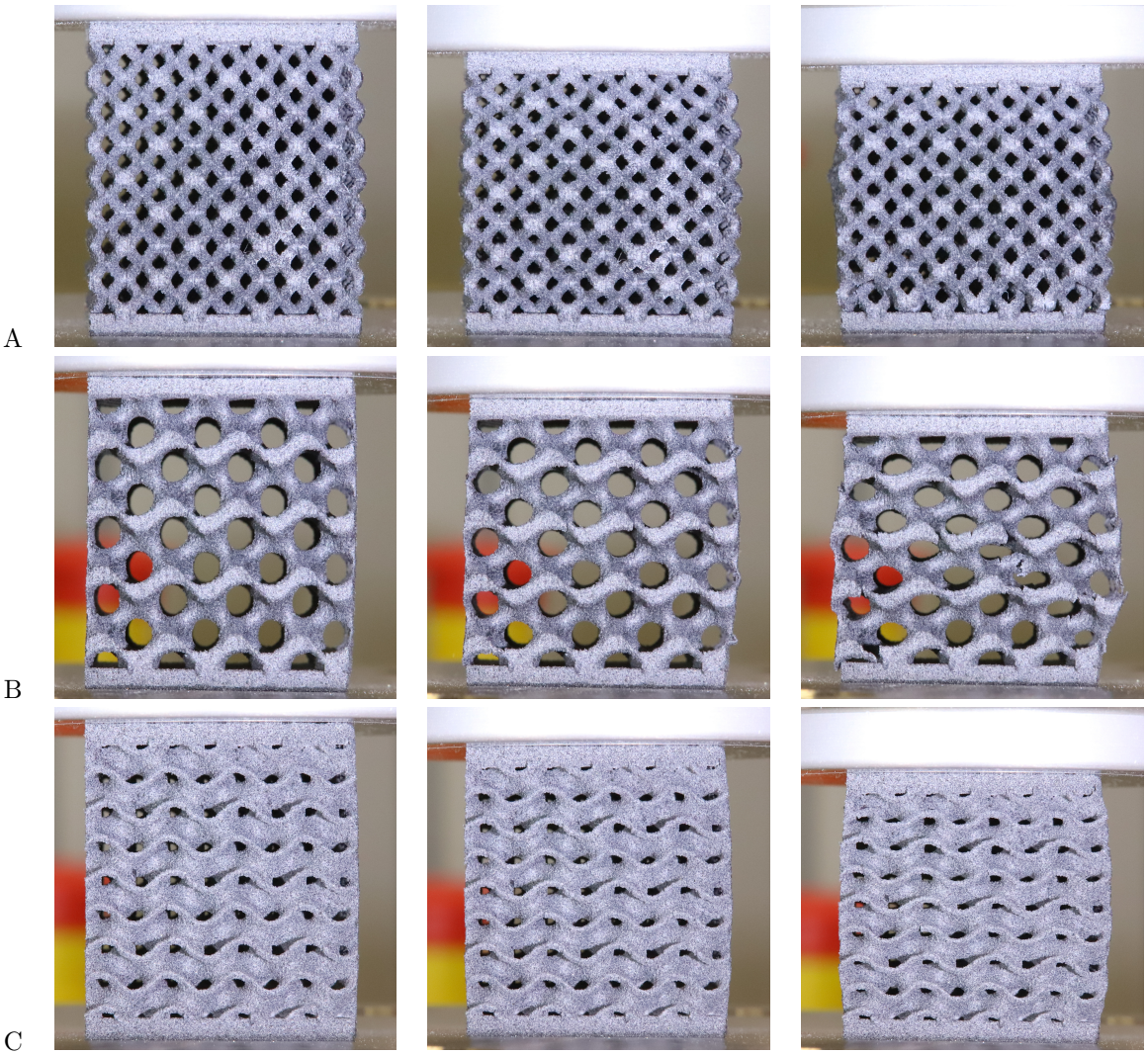

Figure 5. Deformations of specimens during the uniaxial mechanical compression test. Row A – Dode-Thick structure, row B – trabecular gyroid, row C – sheet gyroid. The time of taking the pictures is the beginning of the test (first column), ca. 0.5τ (middle column) and the final time at failure τ (last column).

gyroid structure has $t = 0$ with a CAD-defined wall thickness of 0.5 mm.

The specimens were created using the 3D printer Sinterit Lisa Pro and the PA12 material. Subsequently, they were processed and tested on a pneumatic static press LiTeM. The loading was controlled by displacement with a speed of $0.04\,\frac{\text{mm}}{\text{s}}$. Fig. 5 shows the specimens before and after loading.

2.3. Mesh Generation

For the purpose of 3D printing, it is generally acceptable to use a well-established CAD software for the purpose of generation of the desired geometry, export an *.STL file and prepare it for the printing process. The user usually chooses from a preset variant of the TPMS (triply-periodic minimal surface) structure type (gyroid, linioid, etc.) and specifies the parameters given by the prescribed equation. However, the same is not true if we want to use the geometry for the purpose of FEM analyses as the errors in geometry and tesselation of the output surface are not acceptable (Fig. 6). Therefore, the approach of generating a TPMS surface according to Eq. 1 or Eq. 2 has to be adopted. Subsequently, one domain of the circumscribed cube in which the TPMS surfaces are generated, is enclosed and a solid gyroid structure is created.

3. Results

The results of mechanical tests are shown in Table 1. The values of elastic moduli were calculated from linear parts of load curves obtained via uniaxial compression tests. The specimens before and after load are shown on Fig. 5. From the given figures and tables, we can see that the sheet gyroid variant has much greater stiffness and peak compressive stress (more than double) at the same material density, making it a much more effective variant of material arrangement compared to the Dode-Thick and trabecular gyroid variants. The character of failure (specifically well

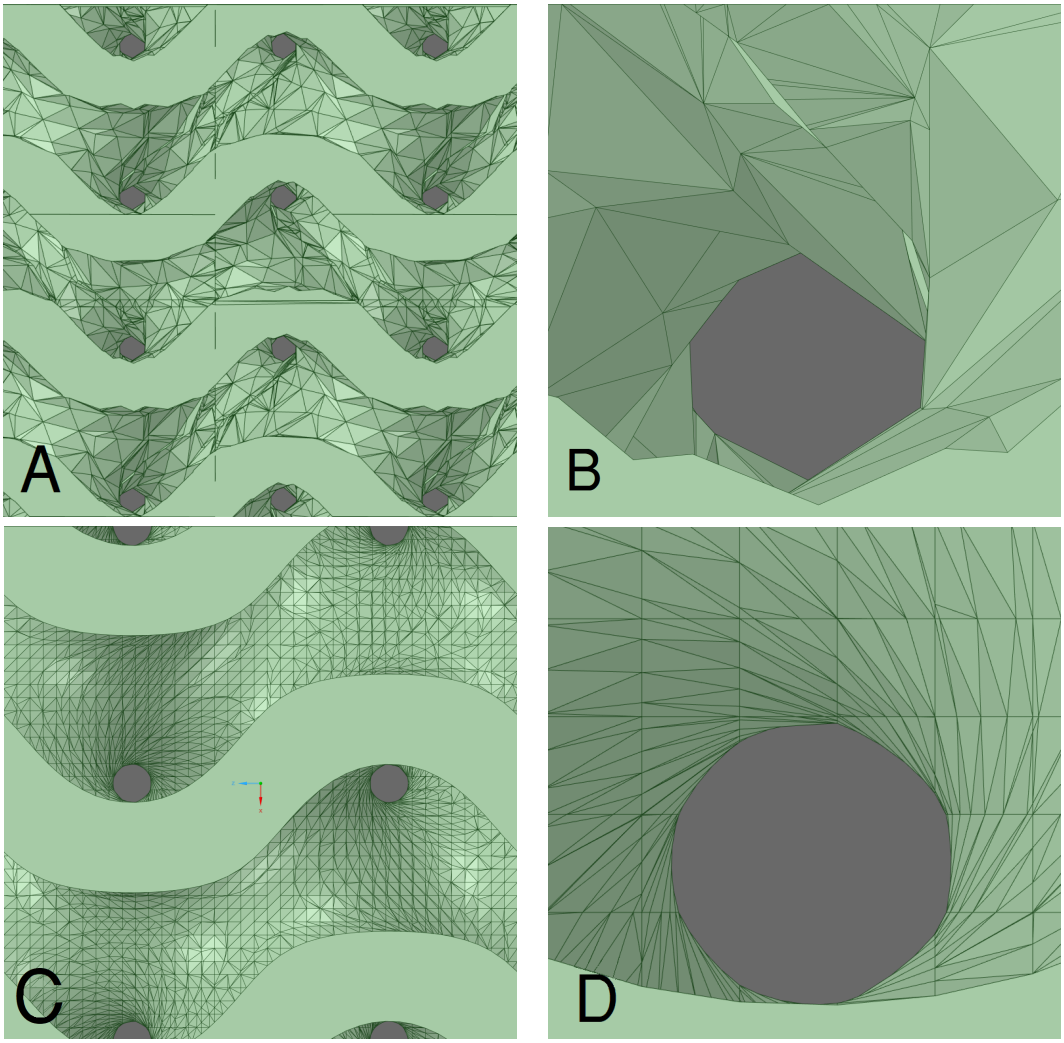

FIGURE 6. A detailed view of gyroid structure models generated via CAD with bad tesselation (A, B) and via modelling with [7] (C, D) and good tesselation. A and C show cutouts of a gyroid structure, B and D show a detailed view. The geometry errors and intersecting small faces make it unable to succesfully generate a FEM mesh, but are good enough for 3D printing. The CAD approach of geometry generation is not suitable for numerical analyses, but sufficient for specimen manufacturing. Variants (C, D) are good enough for FEM.

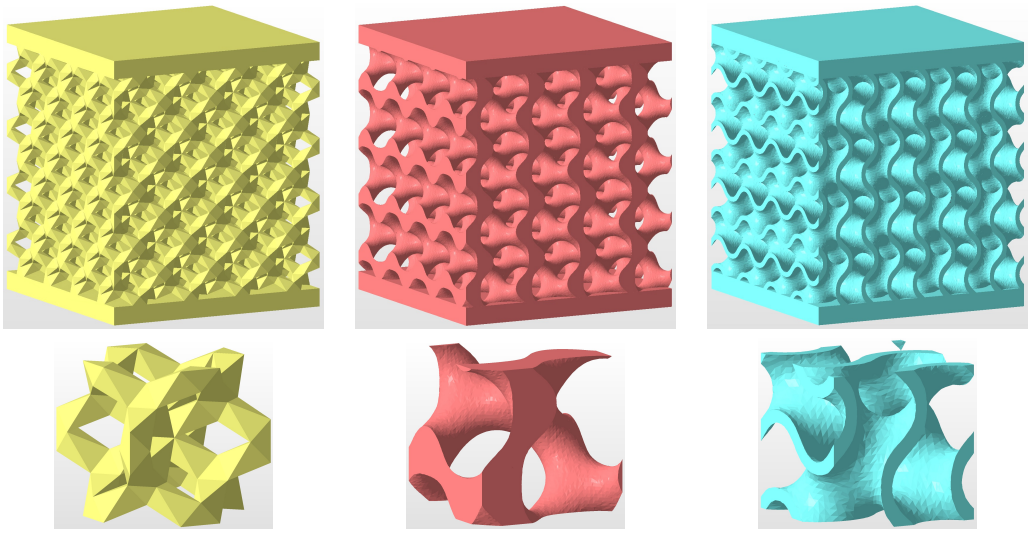

FIGURE 7. Geometry models of specimens for mechanical tests (upper row) and the element basic cells (bottom row). Structures: yellow – Dode-Thick, red – trabecular gyroid, blue – sheet gyroid.

Structure type	$\sigma_{\max}$ [MPa]	E [MPa]
Dode-Thick	1.69 ± 0.25	27.30 ± 3.81
Trabecular gyroid	1.75 ± 0.11	28.74 ± 1.80
Sheet gyroid	4.43 ± 0.47	72.43 ± 6.13

Table 1. Values of maximum peak stress $\sigma_{\max}$ and elastic modulus E of tested trabecular and gyroid structures made from the PA12 material. Values of E obtained from linear parts of load curves of specimens.

captured for the trabecular gyroid structure) can be seen on Fig. 5.

4. Conclusions

The results of this study are twofold – the first part investigated the mechanical properties of gyroid structures manufactured from the PA12 powdered plastic material via SLS. The results are listed in Table 1. Gyroid structures are perspective in the field of implant materials as they represent a porous structure with a system of interconnected pores that is applicable on the surface of an implant. Therefore, the gyroid serves as a medium at the BII, creating greater surface area for ingrowth of bone trabeculae [9], provides sufficient fluid flow for bone remodelling [10] and also provides an interface that diminishes the effects of stress shielding, as it (depending on the structural design) has an elastic modulus in the same order of magnitude as human cancellous bone (in case of Ti-6Al-4V specimens, [11]). Our experiments on PA12 specimens have shown that the sheet gyroid variant has the highest stiffness and peak compressive stress among all variants at the same material density. Reduction of stress shielding, in particular, is a great benefit as many revision surgeries are needed each year [12] because of aseptic loosening and bone loss at the peri-implant area. The difference is apparent, as the values of moduli of human bone are ca. in the range of 1–25 GPa [13], depending on the location in the human body and whether the tissue is trabecular or cortical (trabecular bone occupies the lower range of moduli while cortical bone is stiffer). On the other hand, elastic modulus of common Ti-6Al-4V alloy is ca. 115 GPa and cp-Ti modulus is ca. 105 GPa. The mechanical tests performed on PA12 specimens show that the sheet gyroid structure is much better suited for biomedical applications than trabecular structures with better values of peak stress (Table 1). In the second part, the authors learned that in order to successfully generate a FEM mesh and perform subsequent analyses, it is necessary to use the approach of TPMS generation using the gyroid equations (Eq. 1 and Eq. 2) with subsequent closing of domains and creating solids. The commonly used process for 3D printing, where we create an .STL mesh from a CAD environment, is not applicable for FEM analyses as the intersecting bad quality tesselation impairs the overall geometry quality and prevents the enclosure of a solid body. Performing of the FEM analyses and comparing the moduli obtained from the mechanical tests and simulations is a subject of further research.

Acknowledgements

The financial support provided by the by the Faculty of Civil Engineering, CTU, Prague, project n. SGS20/155/OHK1/3T/11 is gratefully acknowledged.

References

[1] L. Wu, W. Zhang, D. Zhang. Engineering gyroid-structured functional materials via templates discovered in nature and in the lab. *Small* **11**(38):5004–5022, 2015.

[2] A. H. Schoen. *Infinite periodic minimal surfaces without self-intersections*. National Aeronautics and Space Administration, 1970.

[3] R. Ummethala, P. S. Karamched, S. Rathinavelu, et al. Selective laser melting of high-strength, low-modulus ti–35nb–7zr–5ta alloy. *Materialia* **14**:100941, 2020.

[4] G. Yamako, E. Chosa, K. Totoribe, et al. In-vitro biomechanical evaluation of stress shielding and initial stability of a low-modulus hip stem made of β type ti-33.6 nb-4sn alloy. *Medical engineering & physics* **36**(12):1665–1671, 2014.

[5] J. Bobyn, A. Glassman, H. Goto, et al. The effect of stem stiffness on femoral bone resorption after canine porous-coated total hip arthroplasty. *Clinical orthopaedics and related research* (261):196–213, 1990.

[6] H. U. Cameron. The 3—2-6-year results of a modular noncemented low-bending stiffness hip implant: A preliminary study. *The Journal of arthroplasty* **8**(3):239–243, 1993.

[7] O. Al-Ketan, R. K. Abu Al-Rub. Mslattice: A free software for generating uniform and graded lattices based on triply periodic minimal surfaces. *Material Design & Processing Communications* p. e205, 2020.

[8] J. Chin, P. V. Coveney. Chirality and domain growth in the gyroid mesophase. *Proceedings of the Royal Society A: Mathematical, Physical and Engineering Sciences* **462**(2076):3575–3600, 2006.

[9] L. Řehounek, A. Jíra. Experimental and numerical analyses of a 3d-printed titanium trabecular dental implant. *Acta Polytechnica* **57**(3):218–228, 2017.

[10] S. Ma, Q. Tang, Q. Feng, et al. Mechanical behaviours and mass transport properties of bone-mimicking scaffolds consisted of gyroid structures manufactured using selective laser melting. *Journal of the mechanical behavior of biomedical materials* **93**:158–169, 2019.

[11] P. Vakrčka, A. Jíra, P. Hájková. Mechanical testing and numerical modelling of porous structures improving oseintegration of implants. *Acta Polytechnica CTU Proceedings* **26**:126–132, 2020.

[12] C. Chanlalit, D. R. Shukla, J. S. Fitzsimmons, et al. Stress shielding around radial head prostheses. *The Journal of hand surgery* **37**(10):2118–2125, 2012.

[13] H. H. Bayraktar, E. F. Morgan, G. L. Niebur, et al. Comparison of the elastic and yield properties of human femoral trabecular and cortical bone tissue. *Journal of biomechanics* **37**(1):27–35, 2004.